



Environment properties of GRBs with early optical detection

D. Kopač¹, A. Gomboc^{1,2} and J. Japelj¹

¹ Faculty of Mathematics and Physics, University of Ljubljana, Jadranska ulica 19, SI-1000 Ljubljana, Slovenia

² Centre of Excellence SPACE-SI, Aškerčeva cesta 12, SI-1000 Ljubljana, Slovenia
e-mail: drejc.kopac@fmf.uni-lj.si

Abstract. We study the local environment properties of a sample of 26 gamma-ray bursts with early optical detection, among which 8 show possible reverse shock emission. We are particularly interested in intrinsic X-ray column density along the line of sight ($N_{\text{H}}(z)$) and optical extinction in V band (A_{V}). We compare our sample with larger and more general samples and check if presence of the reverse shock emission is somehow related to the surrounding environment.

Key words. gamma-rays: bursts – X-rays: general – dust extinction

1. Introduction

Based on the standard fireball model of gamma-ray bursts (GRBs), optical afterglow is produced when relativistic shell collides with the external medium and decelerates. In this simple scenario, optical light curve of a typical afterglow should be composed of different power-law segments that show shallow rise or decay. We can model the light curve with $F = t^{\alpha}$, where F is flux density and α is power-law index, with typical forward shock indices being $\alpha_{\text{rise}} \lesssim 1/2$ and $\alpha_{\text{decay}} \sim -1$ (Sari, Piran & Narayan 1998). However, at early times, optical light curve can show flares with steep rising and decaying. One mechanism for such behaviour can be the reverse external shock (Sari & Piran 1999), which propagates back into the relativistic shell and decelerates it, producing bright opti-

cal flash in the light curve (Kobayashi 2000), with indices $\alpha_{\text{rise}} \sim 5$ and $\alpha_{\text{decay}} \sim -2$ (Zhang, Kobayashi & Mészáros 2003). In this case, central engines could be magnetized (Zhang, Kobayashi & Mészáros 2003), although the magnetization should not be too large, otherwise it can also suppress the reverse shock emission (Zhang & Kobayashi 2005; Fan, Wei & Wang 2004).

The paucity of observed reverse shock (RS) emission (Gomboc et al. 2009) could be either related to the central engine processes (for example, magnetization), or perhaps to the GRBs' surrounding environment. To examine this possibility, we build a sample of 26 GRBs with early optical detection, among which 8 show possible reverse shock emission. We concentrate on GRBs with known redshifts, observed with *Swift* XRT, to determine the value (or upper limit) of intrinsic X-ray column density. We collect data from the

Send offprint requests to: D. Kopač

Table 1. Sample of 26 GRBs with early optical detection. 8 GRBs show possible reverse shock emission, while for 6 no particular model for optical emission is known from the literature. All $N_{\text{H}}(z)$ values are from Campana et al. (2010), except for values which are marked with ^{a,b,c} and for which the references are: a) Schady et al. (2010); b) the *Swift* XRT GRB lightcurve repository (Evans et al. 2009); c) Pandey et al. (2010). All A_{V} values are from Kann et al. (2010).

GRB	Possible RS	Redshift	$N_{\text{H}}(z)$ [10^{21} cm^{-2}]	A_{V} [mag]	References
050401	no	2.9	$16.4^{+2.2}_{-2.2}$	0.69 ± 0.02	Rykoff et al. (2005)
050525A	yes	0.606	$1.5^{+0.9}_{-0.7}$	0.32 ± 0.20	Klotz et al. (2005)
050820A	no	2.612	$3.4^{+1.3}_{-1.3}$	0.065 ± 0.008	Cenko et al. (2006)
050904	yes	6.29	$63.0^{+34.0}_{-29.0}$	≤ 0.05	Boër et al. (2006); Wei et al. (2006)
051111	no	1.549	$6.0^{+1.9}_{-2.4}$	0.19 ± 0.02	Butler et al. (2006)
060210	no	3.91	$18.9^{+3.4}_{-3.3}$	1.18 ± 0.10	Curran et al. (2007)
060526	not clear	3.221	< 9.8	0.05 ± 0.11	Thöne et al. (2010)
060729	not clear	0.54	$1.4^{+0.2}_{-0.2}$	$0.03 - 0.18$	Grupe et al. (2007)
060904B	not clear	0.703	$4.4^{+0.7}_{-1.2}$	0.08 ± 0.08	Klotz et al. (2008)
060927	no	5.47	< 39	0.209 ± 0.084	Ruiz-Velasco et al. (2007)
061007	no	1.261	$4.5^{+0.3}_{-0.3}$	0.48 ± 0.10	Mundell et al. (2007)
061121	no	1.314	$5.4^{+0.5}_{-0.6}$	$0.28 - 0.55$	Page et al. (2007); Giannios (2008)
061126	yes	1.159	$5.9^{+0.7}_{-0.7}$	0.095 ± 0.055	Gomboc et al. (2008)
070208	no	1.165	$8.6^{+3.0}_{-2.6}$	0.74 ± 0.03	GCN Circulars Archive
080319B	not clear	0.937	$1.3^{+0.1}_{-0.1}$	0.05 ± 0.07	Racusin et al. (2008); Woźniak et al. (2009)
080603A	no	1.688	$6.8^{+2.7}_{-2.5}$	/	Guidorzi et al. (2011)
080721	no	2.591	$7.1^{+0.6}_{-0.6}$	0.35 ± 0.07	Starling et al. (2009)
080810	no	3.35	$4.3^{+2.9}_{-2.3}$	0.16 ± 0.02	Page et al. (2009)
080905B	not clear	2.374	$31.1^{+3.4}_{-5.9}$	/	Ferrero et al. (2010)
080928	not clear	1.692	$3.1^{+1.1}_{-1.0}$	0.14 ± 0.08	Rossi et al. (2010)
090102	yes	1.547	$6.8^{+0.7}_{-1.1}$	/	Steele et al. (2009)
090313	no	3.375	$30.0^{+8.0}_{-7.0}$	0.34 ± 0.15	Melandri et al. (2010)
090424	yes	0.544	$5.1^{+0.4}_{-0.3}$	0.50 ± 0.12	Canizzo et al. (2009)
090902B	yes	1.822	$18.0^{+3.0}_{-3.0}$	0.13 ± 0.04	Pandey et al. (2010)
091024	yes	1.092	$16.0^{+11.0}_{-9.0}$	/	Gruber et al. (2011)
110205A	yes	2.22	$3.8^{+1.3}_{-1.2}$	/	Gao (2011); Cucchiara et al. (2011)

literature, i.e., from Campana et al. (2010) and Evans et al. (2009) for $N_{\text{H}}(z)$, while for A_{V} we use Kann et al. (2010). Data for our sample are presented in Table 1, together with references from which we obtain the information about possible RS emission.

The sample excludes GRBs 990123, 021004, 021211, 041219A, 060111B and

060117, which show possible RS emission, and 050502A, which shows no RS emission. These GRBs were detected in optical at early times after the GRB trigger, but they were excluded from our analysis because either no redshift is known or no $N_{\text{H}}(z)$ could be obtained.

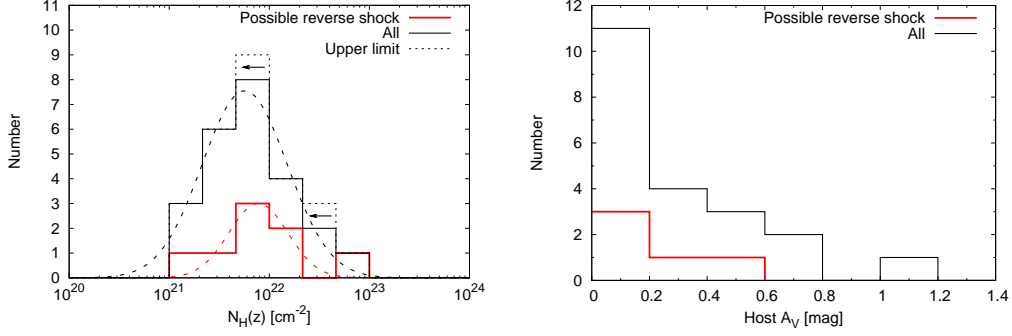


Fig. 1. Left: $N_{\text{H}}(z)$ distribution for our sample. Red color indicates GRBs with possible RS emission, while black color indicates all GRBs from our sample. Also added separately are two upper limits. Red and black dashed lines represent the fitted Gaussian functions in log space, for which the parameters are discussed in the text. Right: A_{V} distribution for our sample. Red color indicates GRBs with possible RS emission, while black color indicates all GRBs from our sample.

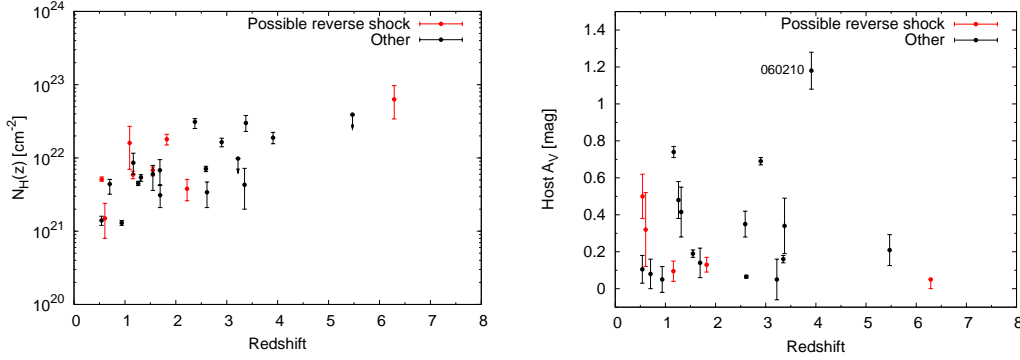


Fig. 2. Left: $N_{\text{H}}(z)$ versus redshift for our sample. Right: A_{V} versus redshift for our sample. Red points indicate GRBs with possible RS emission, while black points indicate all other GRBs from our sample. In the right plot we marked GRB 060210, which has the highest A_{V} , but this value might have been overestimated.

2. Analysis and Discussion

Results are presented in Figure 1, which shows the distributions of $N_{\text{H}}(z)$ and A_{V} for our sample, and in Figure 2, which shows $N_{\text{H}}(z)$ and A_{V} versus redshift. We find that our results are comparable to results for larger samples, i.e., Figure 1 and Figure 2 from Campana et al. (2010) and to Figure 2 and Figure 3 from Kann et al. (2010). We fitted the $N_{\text{H}}(z)$ distribution with a Gaussian function in log space, excluding two upper limits. We get mean $\log N_{\text{H}}(z) = 21.8$ and standard deviation $\sigma_{\log N_{\text{H}}(z)} = 0.4$ (reduced χ^2 of the fit is 0.5 with 3 d.o.f.) for all GRBs from our sample,

while for GRBs that show possible RS emission we get mean $\log N_{\text{H}}(z) = 21.9$ and standard deviation $\sigma_{\log N_{\text{H}}(z)} = 0.3$ (reduced χ^2 of the fit is 0.6 with 3 d.o.f.). These results are comparable to the value of log-normal distribution fit from Campana et al. (2010), with the mean $\log N_{\text{H}}(z) = 21.9$ and standard deviation $\sigma_{\log N_{\text{H}}(z)} = 0.5$. Calculating the median value for A_{V} distribution, we find $A_{\text{V}} = 0.19 \pm 0.14$ mag, which is comparable to the mean value from Kann et al. (2010), who reported the value 0.21 mag for their Golden Sample.

The comparison of $N_{\text{H}}(z)$ and A_{V} for GRBs that show possible RS emission to other GRBs in our sample shows that they tend to have sim-

ilar distributions (Figure 1). The subsample of GRBs with possible RS emission covers a large redshift interval, from $z = 0.54$ to $z = 6.29$. A slight trend of higher $N_{\text{H}}(z)$ at higher z can be seen in the left plot in Figure 2, as already mentioned by Campana et al. (2010) on larger and more general sample. This can also be seen for GRBs without possible RS emission from our sample (excluding the upper limit at $z = 5.47$), although in this case $N_{\text{H}}(z)$ values are a bit more scattered, but they span in redshift only up to $z = 3.91$.

From the right plot in Figure 2 we see that GRBs with possible RS emission tend to have lower A_{V} at higher redshifts, but this can be due to selection bias and small sample size. Anyway, the same trend is not so evident for other GRBs in our sample, which seem to be more scattered in A_{V} versus redshift plot. Note the GRB 060210, which has the highest A_{V} among GRBs in our sample, but as already mentioned by Kann et al. (2010), this extinction might have been overestimated. Kann et al. (2010) noticed on a larger sample that GRBs at higher redshifts tend to have lower A_{V} on average, but they concluded that it is unclear whether this is due to selection effects or due to the evolution of dust properties.

3. Conclusion

Using a sample of GRBs with early optical detections, among which some show possible reverse shock emission, we compare intrinsic X-ray absorption ($N_{\text{H}}(z)$) and host galaxy optical extinction (A_{V}) between GRBs from our sample and GRBs from more general samples, presented in Campana et al. (2010) and Kann et al. (2010). We find no evident discrepancies of host galaxy properties between these samples. This seems to indicate that there are no host galaxy environment differences, and also that the effectiveness of the reverse shock emission is most probably more linked to the central engine processes than to the progenitor's surrounding.

References

Boër, M. et al., 2006, *ApJ*, 638, L71

- Butler, N.R. et al., 2006, *ApJ*, 652, 1390
 Campana, S. et al., 2010, *MNRAS*, 402, 2429
 Canizzo, J.K. et al., 2009, *GCNR*, 221, 1
 Cenko, S.B. et al., 2006, *ApJ*, 652, 490
 Cucchiara, A. et al., 2011, *ApJ*, submitted (arXiv:1107.3352)
 Curran, P.A. et al., 2007, *A&A*, 467, 1049
 Evans, P.A. et al., 2009, *MNRAS*, 397, 1177
 Ferrero, A. et al., 2010, *AdAst*, 2010, ID715237
 Fan, Y.Z., Wei, D.M. & Wang, C.F., 2004, *A&A*, 424, 477
 Gao, W.-H., 2011, *RAA*, accepted (arXiv:1104.3382)
 Giannios, D., 2008, *A&A*, 480, 305
 Gomboc, A. et al., 2008, *ApJ*, 687, 443
 Gomboc, A. et al., 2009, *AIPC*, 1133, 145
 Gruber, D. et al., 2011, *A&A*, 528, 15
 Grupe, D. et al., 2007, *ApJ*, 662, 443
 Guidorzi, C. et al., 2011, *MNRAS*, accepted (arXiv:1105.1591)
 Kann, D.A. et al., 2010, *ApJ*, 720, 1513
 Klotz, A. et al., 2005, *A&A*, 439, 35
 Klotz, A. et al., 2008, *A&A*, 483, 847
 Kobayashi, S., 2000, *ApJ*, 545, 807
 Melandri, A. et al., 2010, *ApJ*, 723, 1331
 Mundell, C.G. et al., 2007, *ApJ*, 660, 489
 Page, K.L. et al., 2007, *ApJ*, 663, 1125
 Page, K.L. et al., 2009, *MNRAS*, 400, 134
 Pandey, S.B. et al., 2010, *ApJ*, 714, 799
 Racusin, J.L. et al., 2008, *Nature*, 445, 183
 Rossi, A. et al., 2010, *A&A*, in press (arXiv:1007.0383)
 Ruiz-Velasco, A.E. et al., 2007, *ApJ*, 699, 1
 Rykoff, E.S. et al., 2005, *ApJ*, 631, L121
 Sari, R., Piran, T. & Narayan, R., 1998, *ApJ*, 497, L17
 Sari, R. & Piran, T., 1999, *ApJ*, 520, 641
 Schady, P. et al., 2010, *MNRAS*, 401, 2773
 Starling, R.L.C. et al., 2009, *MNRAS*, 400, 90
 Steele, I.A. et al., 2009, *Nature*, 462, 767
 Thöne, C.C. et al., 2010, *A&A*, 523, 70
 Zhang, B., Kobayashi, S. & Mészáros, P., 2003, *ApJ*, 595, 950
 Zhang, B. & Kobayashi, S., 2005, *ApJ*, 628, 315
 Wei, D.M., Yan, T. & Fan, Y.-Z., 2006, *ApJ*, 636, L69
 Woźniak, P.R. et al., 2009, *ApJ*, 691, 495